

1 **Supplement**

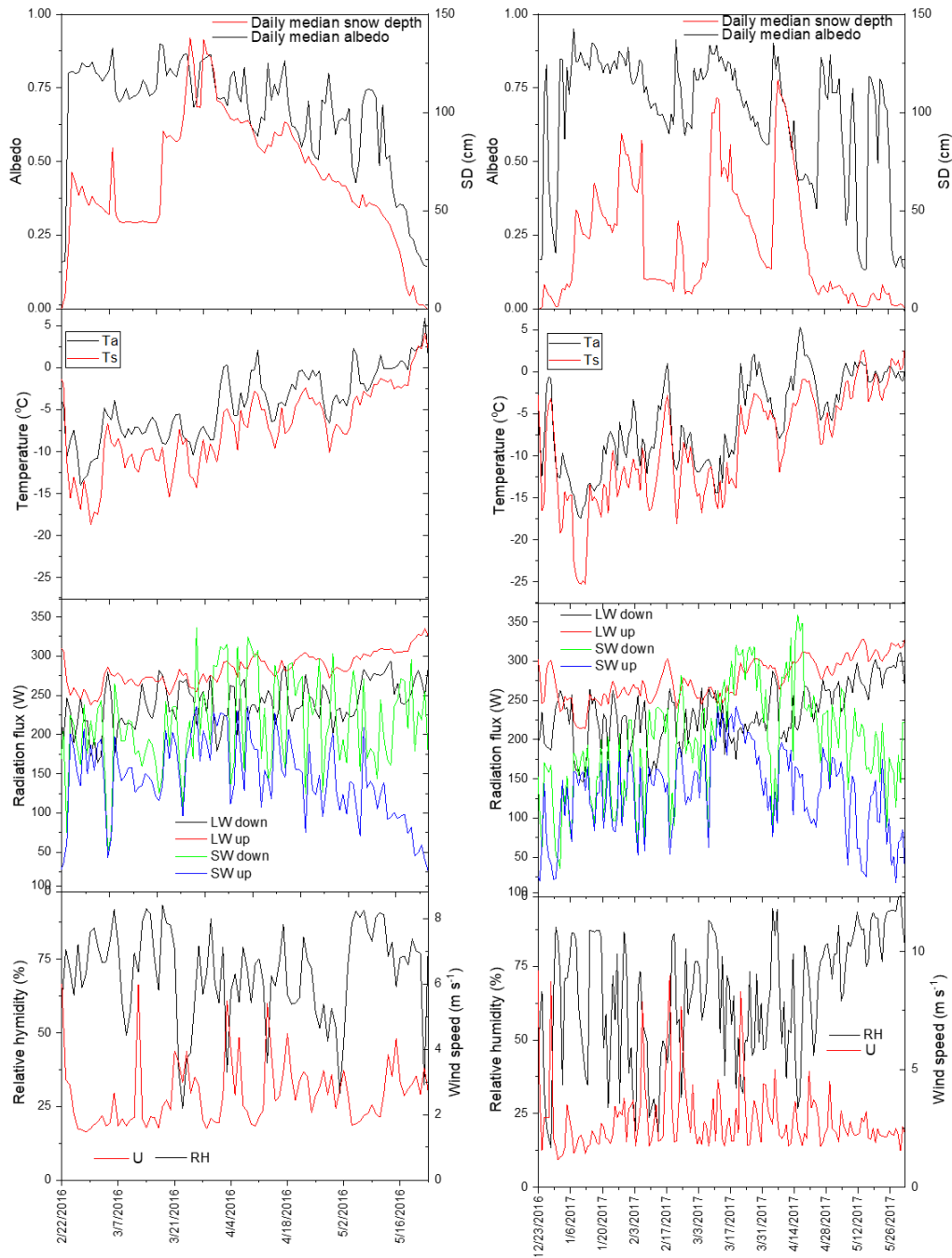
2 1. *Stephan-Boltzmann Law*

3 
$$LW_u = \varepsilon\sigma T^4 \quad (S1)$$

4  $LW_u$  is the broad band long wave radiated energy to the atmosphere (W),  $\sigma = 5.67 \cdot 10^{-8} (W^{-1}m^{-2}K^{-4})$ ,  
5 and T is the temperature (K). The emissivity,  $\varepsilon=1$ .

6 2. *AWS data*

7 Figure S1 shows the important variables used in this study. Unfortunately, pressure was not operational in  
8 Season 1 and instead a constant value based on the average over Season 2 was used in the turbulent flux  
9 estimates below.

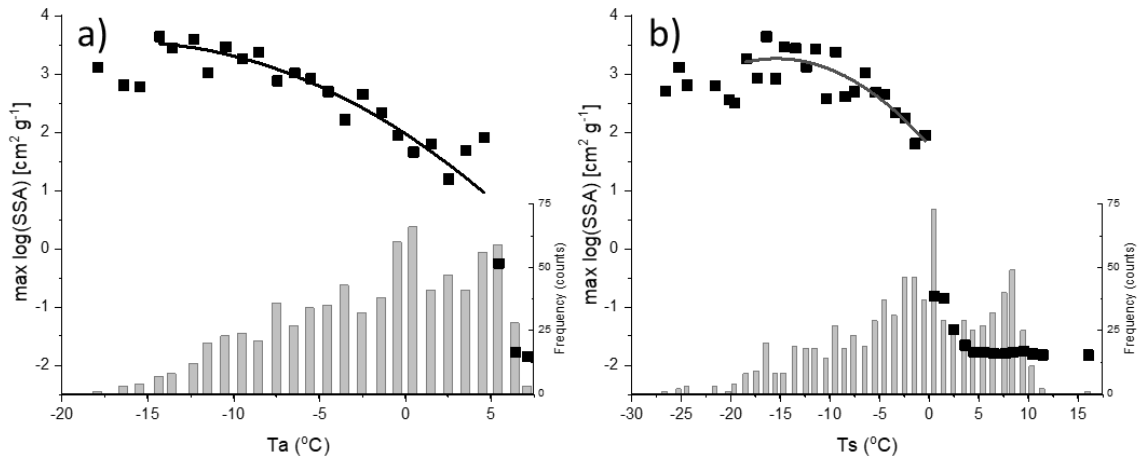


10

11 Figure S1. Data from Season 1 is presented in the column to the left and data from Season 2 is presented in the  
 12 column to the right. Variables presented are noted in each frame.

13 *3. Fitted expressions between maximum log(SSA) and,  $T_a$  or  $T_s$ .*

14 Data is presented in Figure S2. The number of data points at the very coldest temperatures are very few and are  
 15 probably not representative. These data points correspond to a few days of enhanced cooling due to negative  
 16 radiation balance, and do not represent the pristine snow characteristics.



17

18 Figure S2. All data covering the whole measuring period are used to generate Figure S2. In frame a) data is  
 19 classified according to air temperature. In frame b) data is classified according to surface temperature. Symbols  
 20 are the logarithm of the maximum SSA ( $\text{cm}^2 \text{g}^{-1}$ ) in each temperature bin. The SSA value is calculated using  
 21 equation 2 in the main text as function of observed daily median albedo. The histograms show the number of  
 22 data points in each bin. The solid lines are the respective fitted curves presented in equation S2 and S3. The  
 23 extent of the lines show over which domain the fits were made (-15 to +5 °C for  $T_a$  and -19 to 0 °C for  $T_s$ ).

$$24 \quad \log(\text{SSA}) = -5.92 \cdot 10^{-3} T_a - 0.193 T_a + 1.97 \quad (\text{S2})$$

$$25 \quad \log(\text{SSA}) = -6.32 \cdot 10^{-3} T_s - 0.195 T_s + 1.76 \quad (\text{S3})$$

26

27 Below we provide a discussion on air temperature ( $T_a$ ), but believe that the same reasoning is applicable to  $T_s$ .  
 28 For a given daily average temperature, equation 3 provides the estimated SSA of the brightest snow surface  
 29 albedo based on two seasons of data. Those events are thought to occur for relatively young snow without  
 30 significant influence from LAP. However, this empirical relation will provide the same albedo for young snow  
 31 at a given daily temperature as for snow that fell at an earlier instance, but with a different temperature for a  
 32 particular day. After snowfall, the temperature either increased or decreased. Because eq. 3 only depends on the  
 33 average temperature of the day, this memory effect is not captured by the parameterization.

34 Because the relation is already based on maximum albedos at a given daily temperature (decreasing trend with  
 35 increasing temperature), it is not likely that a snow surface at a given temperature will maintain a high albedo  
 36 to a future day with a warmer temperature. However, it could conceivably be lower than predicted by the  
 37 formulation due to metamorphism. Hence, in an environment with increasing temperatures our parameterization  
 38 represents the upper range of possible SSA for a given temperature and may overestimate SSA of pristine snow  
 39 for a given temperature. The same is also true for environments where the temperature is decreasing. In this  
 40 case, snow at a given temperature may maintain or lower the SSA as the temperature decreases, but not likely  
 41 increase the SSA above the value given by the parameterization. It is possible that this effect is visible at the  
 42 very coldest temperatures (c.f. Figure S2) and that the observed lower albedo is actually an effect of snow  
 43 arriving at some significantly warmer temperature (e.g. lower albedo). Clear skies (no additional precipitation)  
 44 and radiative cooling lower the temperature while maintaining the same snow on top. The general over-  
 45 estimation of the albedo (under-estimation of accumulated energy) in at the beginning of the seasons (c.f. Figure  
 46 5), could be a result of this combination of events. From Figure 5, there are small changes in accumulated energy  
 47 due to changes in LAP deposition. This indicates that the difference between observed accumulated energy and  
 48 the estimated values, mainly arrive from the simplicity of eq. 3.

49 In either case, our empirical relation should be considered an upper estimate of pristine snow SSA. Assuming  
 50 that our estimates are consistently a factor of two too high, we can estimate the effect by simply divide our  
 51 derived SSA with a factor 0.5. Reducing SSA will reduce the pristine snow albedo according to equation 2.  
 52 Reducing SSA will also reduce  $r_e$ , (c.f. equation 1), which in turn will affect the absorption by LAP via equations  
 53 5 and 4. We can assess the overall impact by comparing the observed albedo and the parameterized albedos  
 54 with and without the factor 0.5 (see table S1). The largest impact on the change in albedo from changing SSA  
 55 is via  $r_e$  in the LAP parameterization (eq. 4 and 5). The net effect of changing SSA by a factor of two is about 6  
 56 percent-units on the average albedo or a relative change of about 10 % for both seasons, see Table S1.

57 Table S1.

Season 1				Season 2			
	SSA*1	SSA*0.5			SSA*1	SSA*0.5	
Observed average albedo	Derived average albedo	Derived average albedo	Percentage change between different SSA	Observed average albedo	Derived average albedo	Derived average albedo	Percentage change between different SSA
0.67	0.69	0.63	9	0.66	0.67	0.61	9

58

59

60 4. Parametric relation proposed by Pedersen et al. (2015)

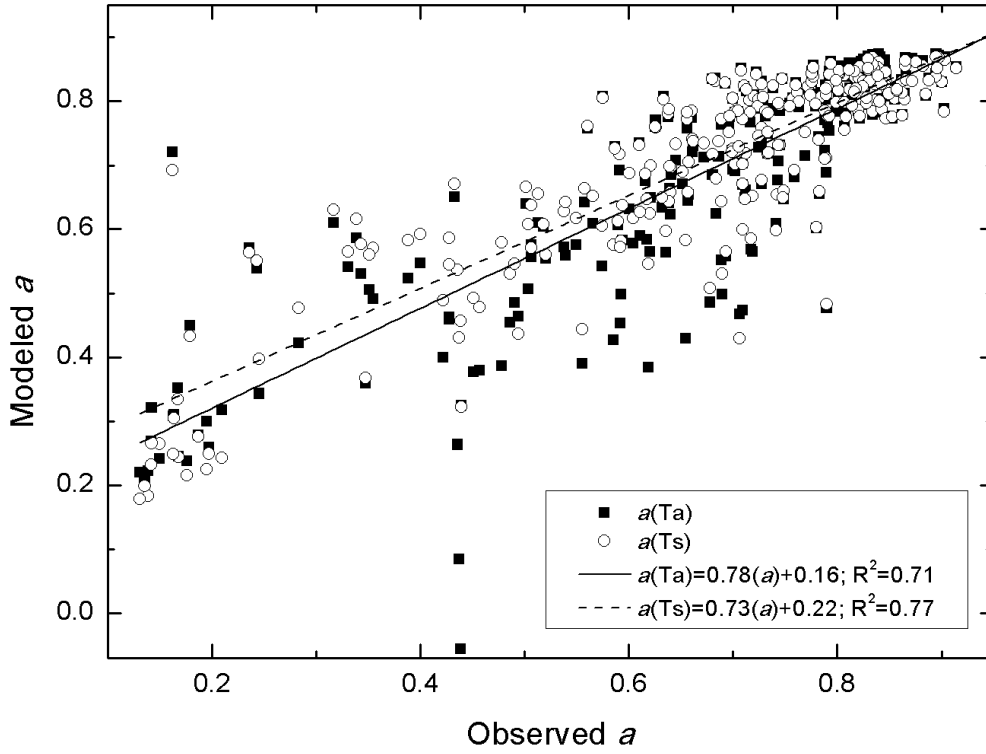
61 Parameters A, B, and C used in equation 4 of the main text have the form  $A(\lambda) = a\lambda^2 + b\lambda + c$ , where  $\lambda$  is the  
 62 wavelength in nanometer between 400-900 nm.

63 Table S1

	a	b	c
A( $\lambda$ )	-3.5e-7	2.7e-4	0.95
B( $\lambda$ )	1.9e-8	-2.0e-5	0.0062
C( $\lambda$ )	-4.0e-7	3.5e-4	0.45

64

65 5. Comparison between the observed albedo and  $a(T_a)$  and  $a(T_s)$  including wag for the two seasons put  
 66 together.



67  
68 Figure S3. The parameterized albedo using both  $T_a$  and  $T_s$  as a function of the observed albedo for all of the  
69 data points from the two seasons.

70  
71 6. *Estimates of turbulent energy fluxes*

72 We have used the same set of equations as used in many other studies (e.g. Boudhar et al., 2016) to estimate the  
73 sensible ( $H$ ) and latent ( $LE$ ) heat fluxes. The equations used are provided below. Here  $\rho$  is the air density,  $C_p$  is  
74 the heat capacity of air,  $L_s$  is the latent heat of sublimation,  $k$  is the von Karman constant,  $u$  is the wind speed,  
75  $T_a$  and  $T_s$  are the air and surface temperatures, respectively. The specific humidities of air ( $q_a$ ) and at the surface  
76 ( $q_s$ ) are calculated using the observed RH and the saturation vapour pressure according to Buck (1981) and  
77 assuming saturation conditions over the snow surface. The distance between the AWS sensors and the snow  
78 surface is  $z$ , which varies over the season. The surface roughness length  $z_{0m}$  is set to a constant value of  $10^{-3}$ ,  
79 and  $z_{0T} = z_{0q} = 10^{-1}z_{0m}$ .

80 
$$H = \rho \frac{C_p k^2 u (T_a - T_s)}{\ln\left(\frac{z}{z_{0m}}\right) \ln\left(\frac{z}{z_{0T}}\right)} (\Phi_m \Phi_h)^{-1} \quad (S4)$$

81 
$$LE = \rho \frac{L_s k^2 u (q_a - q_s)}{\ln\left(\frac{z}{z_{0m}}\right) \ln\left(\frac{z}{z_{0q}}\right)} (\Phi_m \Phi_v)^{-1} \quad (S5)$$

82 The non-dimensional stability adjustment parameters for momentum ( $\Phi_m$ ), for vapour ( $\Phi_v$ ), and for heat ( $\Phi_h$ )  
83 depend on the Richardson number,  $R_{ib}$ .

84 For neutral conditions  $R_{ib} = 0$

85 
$$(\Phi_m \Phi_v)^{-1} = (\Phi_m \Phi_h)^{-1} = 1$$

86 For stable conditions  $R_{ib} > 0$

87 
$$(\Phi_m \Phi_v)^{-1} = (\Phi_m \Phi_h)^{-1} = (1 - 5R_{ib})^2 \quad (S6)$$

88 For unstable conditions  $R_{ib} < 0$

89 
$$(\phi_m \phi_v)^{-1} = (\phi_m \phi_h)^{-1} = (1 - 16R_{ib})^{0.75} \quad (S7)$$

90 The Richardson number is estimated according to:

91 
$$R_{ib} = \frac{g(T_a - T_s)(z - z_{om})}{T_a u^2} \quad (S8)$$

92 where  $g$  is the gravity constant.

93

94

95

96

97

98

99 References Supplement

100 Buck, A. L. (1981), New equations for computing vapor pressure and enhancement factor, J. Appl. Meteorol.,  
101 20: 1527–1532.

102 Boudhar, A, Bouletb, G., Hanichc, L., Sicartd, J.-E., Chehbounib, A. (2016), Energy fluxes and melt rate of a  
103 seasonal snow cover in the Moroccan High Atlas, Hydro. Sc. J., 61, 931–943.

104

105